*Friction* **8**(6): 1051–1062 (2020)
https://doi.org/10.1007/s40544-019-0318-y
ISSN 2223-7690
CN 10-1237/TH
RESEARCH ARTICLE

# Assessment of water-based cutting fluids with green additives in broaching

**Jing NI, Kai FENG, Lihua HE*, Xiaofan LIU, Zhen MENG**
*School of Mechanical Engineering, Hangzhou Dianzi University, Hangzhou 310018, China*
*Received: 09 January 2019 / Revised: 28 May 2019 / Accepted: 09 July 2019*


**Abstract:** In order to improve the cutting performance in broaching, the lubrication and cleaning effects offered by water-based cutting fluids with green additives need to be studied from the viewpoint of green manufacturing. Therefore, water-based solutions with castor oil, surfactant (linear alkylbenzene sulfonate, LAS), and nanographite were prepared by ultrasonic agitation and sprayed into the zone of broaching via atomization. The performances of the cutting fluids, in terms of the viscosity, specific heat, wetting angle, and droplet size, were evaluated to discuss their effects on the broaching load. Among the fluids, the addition of LAS into oil-in-water (WO-S), where its cutting fluid with 10 wt.% castor oil and 1.5 wt.% surfactant, exhibited the lowest broaching force. With regard to the lubricating and cleaning mechanisms, WO-S has good wettability and permeability, and hence, can lubricate the cutting edge of the tool to decrease the cutting load, cool the cutting edge to keep it sturdy, and clean the surface of the cutting edge to keep it sharp. The results reveal that the simultaneous addition of castor oil and LAS had remarkable effects on the lubrication and cleaning, and resulted in a broaching load reduction of more than 10% compared to commercial cutting fluids. However, the addition of nanographite could not improve the lubrication owing to its agglomeration.

**Keywords:** cutting fluid; castor oil; linear alkylbenzene sulfonate; nanographite; broaching

## 1 Introduction

Broaching is an efficient and fine cutting process, and is widely used in the aerospace, automobile, vessel, and energy industries. Owing to the heavy cutting load (at least 10 kN) in broaching process, research to identify suitable coolant lubricants is imperative to reduce the broaching temperature and friction, and thereby improve the tool life and machining quality.

However, the traditional metal working fluid (MWF), which is mineral oil containing lubricants, is difficult to degrade, and can hence cause severe environmental pollution [1]. Moreover, it consists of toxic additives such as preservatives, wetting agents, fungicides, and extreme pressure agents, which can cause illness like lung cancer, respiratory diseases, dermatological diseases, and genetic diseases when inhaled or injury when splashed on the skin of workers [2, 3]. Therefore, since the past few decades, research interest in the field of water-based cutting fluids with green additives or methods for their similar multifarious applications is increasing.

Currently, vegetable oils, which are biodegradable non-toxic compounds in nature, are emulsified as additives in water-based cutting fluids for use as anti-wear agents [4]. In some applications, vegetable oils have been reported to reduce the friction. Xavior and Adithan [5] confirmed that coconut oil performs better than an emulsion and neat cutting oil in turning. Similarly, Sarıkaya and Güllü [6] observed that vegetable oil could decrease the tool wear to its lowest, and had immense potential in turning. When applied in drilling, reaming, and tapping to machine AISI 316L specimens, vegetable-oil-based cutting fluids reduced the built

* Corresponding author: Lihua HE, E-mail: helihua0617@yahoo.com

up edge (BUE); their performance for the same was comparable to or better than mineral oils after cutting force tests [7, 8]. Water is an inexpensive, pollution-free, eco-friendly, and safe lubricant. The development of water-based lubricants with vegetable oils has now emerged as a primary research area. Burton et al. [9] developed a stable emulsion of vegetable oil in water which could lower the cutting forces, chip thickness, and burr amount during milling operations. Li and Wang et al. [10, 11] used seven vegetable oils in water and compared their different advantages in terms of the grinding force, grinding temperature, and energy ratio coefficient. Furthermore, Shokoohi et al. [12] proposed an eco-friendly cutting fluid with water-mixed vegetable oil that could potentially enhance the productivity of cutting operations in terms of the machining quality, costs, operator health, and environmental protection.

Surfactants and emulsions exhibit outstanding surface activity. Bataller et al. [13] produced a relatively stable emulsion with submicron-sized oil droplets, that allowed the user to fine-tune the lubricating and cooling abilities of the fluids for optimizing the performances in metal machining. Cambiella et al. [14] evaluated the effect of the concentration of three different emulsifiers (anionic, non-ionic, and cationic surfactants) on the extreme pressure properties of oil-in-water emulsions in machining operations. John et al. [15] demonstrated that a certain concentration of surfactant could help accelerate the formation of a more stable emulsion and improve its performance. Adamczuk et al. [16] observed a reduction in the roughness parameter Ra on a workpiece surface and an improvement in the durability of a pull broach upon modifying metal machining oil with an active additive during broaching. Sukirno and Ningsih [17] showed that the surface roughness, bearing capacity, and extreme pressure properties of palm oil with a sulfurized additive were significantly improved in broaching. Krishna et al. [18] added boric acid granules to SAE-40 oil and coconut oil.

Nanoparticles have been employed in lubrication. Nanolubricants can be formed from a colloidal dispersion of nanoparticles in a cutting fluid. Coconut oil with a nanoparticle suspension performed better than SAE-40 oil in terms of the cutting temperature, flank wear, and surface finish. Solid nanoparticles can also potentially play a beneficial role. Zareh-Desari and Davoodi [19] proved that adding a proper concentration of $SiO_2$ and CuO nanoparticle additives into soybean and rapeseed oil could lead to significant friction reduction. Chu et al. [20] observed that the cutting force decreased to its lowest and then increased when using a canola-oil-based fluid with different concentrations of graphene platelets (GPLs) in micro-turning. In addition, Ni et al. [21] mixed graphene additives into pure vegetable oils with different concentrations to analyze their tapping performances.

Minimum quantity lubrication (MQL), the consumption reduction compared to conventional flood cooling style, is regarded as a "green" application technology. Maruda et al. [22] showed that MQL technology could improve the penetration of lubricants by atomizing a small amount of cutting fluid with a certain pressure of air and spraying it into the cutting zone. Uysal et al. [23] found that MQL technology could lead to minimum tool wear and surface roughness in milling. Moreover, Klocke et al. [24] showed MQL technology improved the surface finish and tool life, and also reduced the machining forces.

Despite the numerous experimental studies thus far on green cutting fluids, their use in broaching has rarely been reported because of its sealing and high load. Therefore, this study focuses on the lubrication performance of water-based cutting fluids with green additives, such as castor oil, surfactant (linear alkylbenzene sulfonate, LAS) and nanographite, in broaching. The broaching load is compared for commercial cutting oil and three types of MWF under MQL. Moreover, the effects of different proportions of additives on the physical properties of the MWF are studied to identify the optimal MWF for broaching. Finally, the lubricating and cleaning mechanisms are analyzed using the obtained results.

## 2 Experimental setup

### 2.1 Experimental system for broaching

Figure 1 shows the horizontal internal broaching machine (Changer LG612Ya-800) used in this study. The machine tool parameters were a constant broaching force of 20 kN, maximum broaching stroke of 800 mm, rated broaching speed of 80 mm/s, and broaching time for each workpiece of 8 s. A master cylinder of size

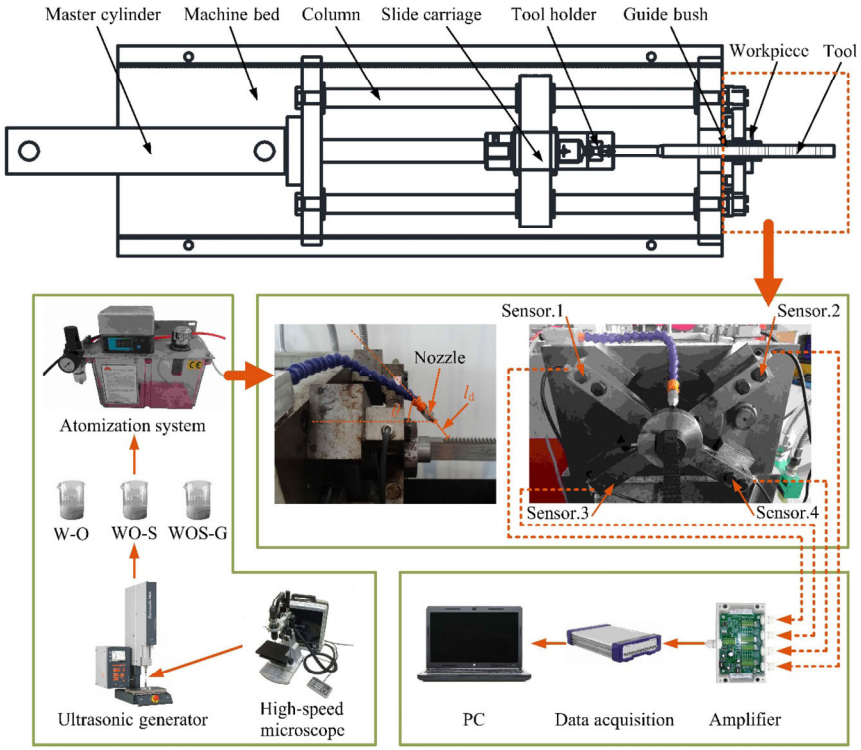


**Fig. 1** Experimental setup for broaching.

Ø80 mm×45 mm–800 mm (80 mm shows the outside diameter of the master cylinder, 45 mm is the the crown diameter of piston, and 800 mm represents the piston stroke length) was used as the control device to regulate the oil pressure of 6 MPa and flow of 100 L/min.

The experimental setup for broaching (Fig. 1) mainly consists of a force transducer, data acquisition instrument, and microscope. The force transducer, which is composed of four pressure sensors (CTY-204) and one amplifier, was employed for detecting the broaching force with a maximum output voltage of 10 V, maximum load of 2 t, voltage sensibility of 2 mV/V, precision of 0.001, and frequency response of 50 Hz. The data acquisition instrument (INV3018CT) was used for the sample data with sample software (CIONV DASP V10). It was operated with a sampling frequency of 1 kHz and a sampling precision of 24 bit. A high-speed microscope (KEYENCE VW9000) was used to observe and analyze the contact angle (where the cutting fluid interface meets the broach and workpiece surface).

## 2.2 Broaching tool and workpiece

### 2.2.1 *Broaching tool set up*

As shown in Fig. 2, the broaching tool is made from HSS-6542 steel, and has a length ($L$) of 600 mm, width ($b$) of 16 mm, front height ($h_1$) of 35.10 mm, and rear height ($h_{50}$) of 36.75 mm. The maximum tooth number on the tool is indicated by $n_m$. Moreover, there are roughing, semi-finishing, and finishing cutting teeth zones on one broaching tool. $n_R$ represents the number of roughing teeth; $n_S$, the number of semi-finishing teeth; and $n_f$, the number of finishing teeth. In this experimental system, $n_R = 40$, $n_S = 5$, $n_F = 5$, and $n_m = 50$. Table 1 lists the cutting depth ($\delta_i$) of every tooth on the tool. Each tooth has a rake angle ($\gamma_0$) of 12°, clearance angle of 6°, and pitch ($p$) of 6 mm.

### 2.2.2 *Workpiece set up*

The experimental workpiece is a cylinder of 1045(AISI) steel, as shown in Fig. 2. The dimensions of the workpiece are 90 mm in outside diameter (ED), 41 mm in inner diameter (ID), and 20 mm in thickness ($l_W$). The total cutting depth ($\delta_m$) is approximately 1.88 mm.

## 2.3 Preparation of cutting fluids

In this study, three types of water-based cutting fluids were prepared based on their outstanding performances in terms of lubrication, cooling, and cleaning. As

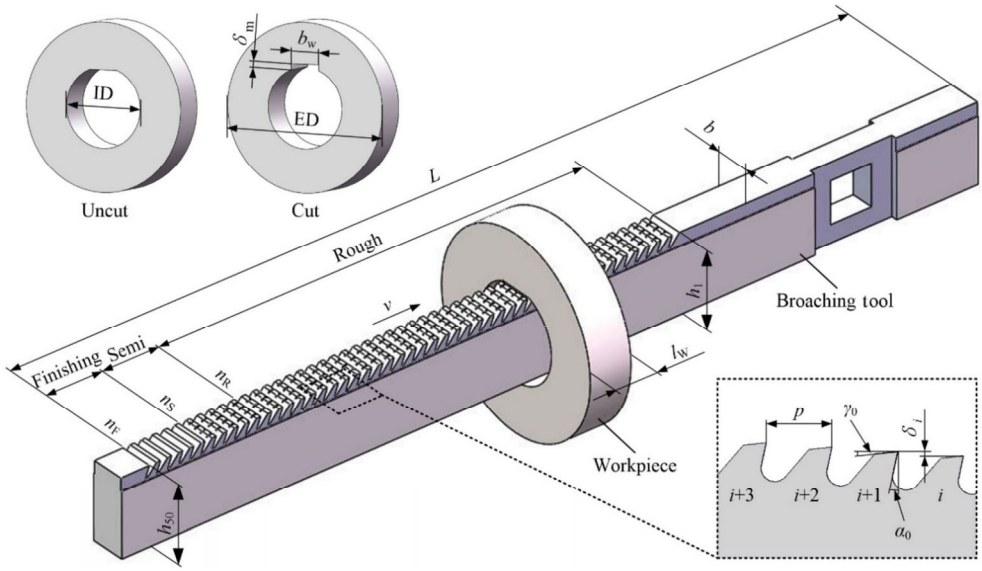


**Fig. 2** Schematic diagram of tool and workpiece.

**Table 1** Rise per tooth in different zone on broach.

| No.*i* | $\delta_i$ | Zone | No.*i* | $\delta_i$ | Zone |
|---|---|---|---|---|---|
| 1 | 0.04 | Rough | 26 | 0.04 | Rough |
| 2 | 0.04 | Rough | 27 | 0.04 | Rough |
| 3 | 0.04 | Rough | 28 | 0.04 | Rough |
| 4 | 0.04 | Rough | 29 | 0.04 | Rough |
| 5 | 0.04 | Rough | 30 | 0.04 | Rough |
| 6 | 0.04 | Rough | 31 | 0.04 | Rough |
| 7 | 0.04 | Rough | 32 | 0.04 | Rough |
| 8 | 0.04 | Rough | 33 | 0.04 | Rough |
| 9 | 0.04 | Rough | 34 | 0.04 | Rough |
| 10 | 0.04 | Rough | 35 | 0.04 | Rough |
| 11 | 0.04 | Rough | 36 | 0.04 | Rough |
| 12 | 0.04 | Rough | 37 | 0.04 | Rough |
| 13 | 0.04 | Rough | 38 | 0.04 | Rough |
| 14 | 0.04 | Rough | 39 | 0.04 | Rough |
| 15 | 0.04 | Rough | 40 | 0.04 | Rough |
| 16 | 0.04 | Rough | 41 | 0.02 | Semi |
| 17 | 0.04 | Rough | 42 | 0.02 | Semi |
| 18 | 0.04 | Rough | 43 | 0.01 | Semi |
| 19 | 0.04 | Rough | 44 | 0.01 | Semi |
| 20 | 0.04 | Rough | 45 | 0.01 | Semi |
| 21 | 0.04 | Rough | 46 | 0 | Fine |
| 22 | 0.04 | Rough | 47 | 0 | Fine |
| 23 | 0.04 | Rough | 48 | 0 | Fine |
| 24 | 0.04 | Rough | 49 | 0 | Fine |
| 25 | 0.04 | Rough | 50 | 0 | Fine |

shown in Table 2, the first type of cutting fluid is prepared by adding oil into water (designated as W-O, where W represents water and O is oil). There are five variants of the W-O cutting fluid depending on different oil contents. The second type of cutting fluid is designated "WO-S", and is prepared by the addition of LAS (represented by S) into the optimal W-O. Here too, there are five variants of WO-S depending on different LAS concentrations. To further optimize the second type of cutting fluid, "WOS-G", prepared by the addition of nanographite into the ideal WO-S, represents the third type of cutting fluid. Here, G represents nanographite, the particle size of which is approximately 50 nm. However, only four variants of WOS-G with different percentages of nanographite are compared. Finally, a commercial cutting fluid (CCF) is used for comparison.

In the preparation of all three types of cutting fluids, a 2,400 W probe sonicator (CH-8590, Rinco, Switzerland) was used to sufficiently enhance the fluid mixing down to the nanometer scale. As shown in Fig. 1, the cutting fluids were ultrasonically agitated by a vibrating probe at high frequency (20 kHz) for 5 min. During operation, the temperature was controlled using a water bath. Finally, the cutting fluids were left for 3 min until they were stable.

The viscosities of the three types of cutting fluids were measured using a SYD-265B-I kinematic viscometer, the densities were measured from the mass

**Table 2** Configuration of three types of cutting fluids.

| Types | Water (wt.%) | Castor oil (wt.%) | Surfactant (wt.%) | Nanographite (wt.%) |
|---|---|---|---|---|
| W-O | 99 | 1 | — | — |
| | 95 | 5 | — | — |
| | 90 | 10 | — | — |
| | 85 | 15 | — | — |
| | 80 | 20 | — | — |
| WO-S | 89.5 | 10 | 0.5 | — |
| | 89 | 10 | 1 | — |
| | 88.5 | 10 | 1.5 | — |
| | 88 | 10 | 2 | — |
| | 87.5 | 10 | 2.5 | — |
| WOS-G | 88.25 | 10 | 1.5 | 0.25 |
| | 88 | 10 | 1.5 | 0.5 |
| | 87.75 | 10 | 1.5 | 0.75 |
| | 87.5 | 10 | 1.5 | 1 |

and volume, and the specific heats were measured using the H131148 Liquid Specific Heat Capacity Tester. Moreover, contact angles of the cutting fluids on the broaching tool and workpiece were measured using a KEYENCE VW-9000 high-speed microscope that could capture images at the rate of 23000 frames per second. Microscopic observation of the droplets of the three types of cutting fluids was conducted using the metallographic microscope OLYMPUS-BX53M with 1000× magnification.

### 2.4 Atomization of cutting fluids

With a TZ-2232-ASPP pump in an atomization injection system, the cutting fluids were sprayed into the cutting zone (Fig. 1). Here, the maximum storage volume of the cutting fluids was 3 L and maximum injection flow rate was 16 mL/min. An atomization nozzle with a working gas pressure of 7 bar was applied to deliver the cutting fluids into the cutting zone between the tool and workpiece. A ramp angle ($\theta$) of 15° and a distance ($l_d$) of 50 mm were used for the atomization nozzle to obtain the best lubrication and cooling.

## 3 Results and discussion

### 3.1 Broaching load with cutting fluids

The broaching load is an important factor in evaluating the lubrication performance of cutting fluids. Five repetitive broaching experiments were performed on each different cutting fluid. Data from one experiment were then randomly selected. The broaching load under the three types of cutting fluids was measured and is shown in Figs. 3–5. As the thickness ($l_W$) of the workpiece was 20 mm and the pitch ($p$) of the teeth was 6 mm, i.e., $l_W > 3p$, the number of teeth engaged in cutting varied between 3 and 4 during broaching. The broaching load was high for cutting by four teeth and low for cutting by three teeth. Hence, there would be several high and low values in one pass of the broach. Therefore, the mean high and low values were calculated.

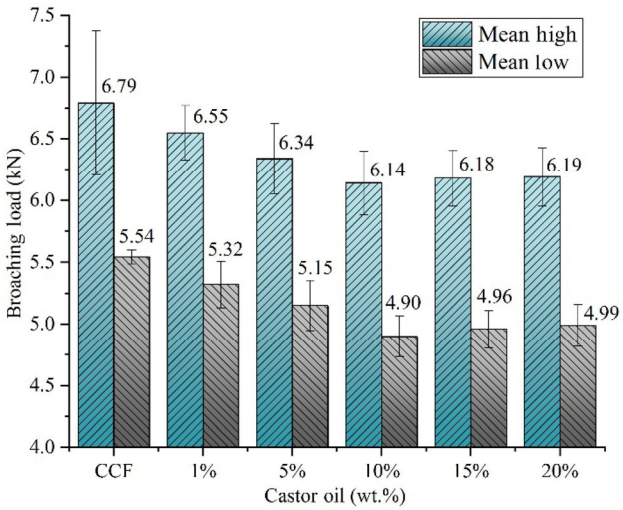


**Fig. 3** Broaching load for different concentrations of castor oil in the W-O cutting fluid.

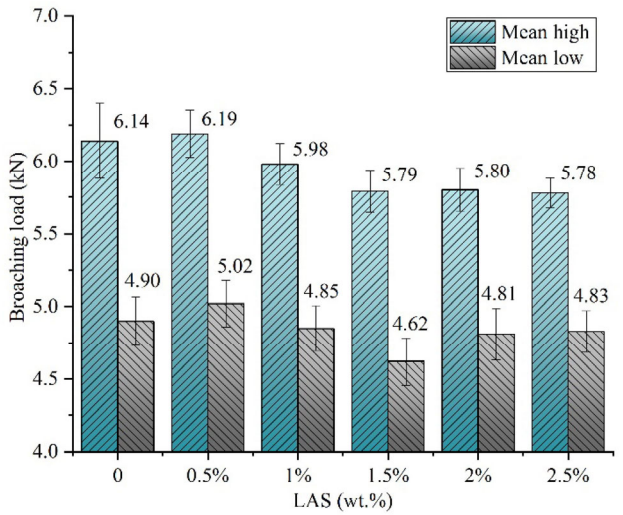


**Fig. 4** Broaching load for different concentrations of LAS in the WO-S cutting fluid.

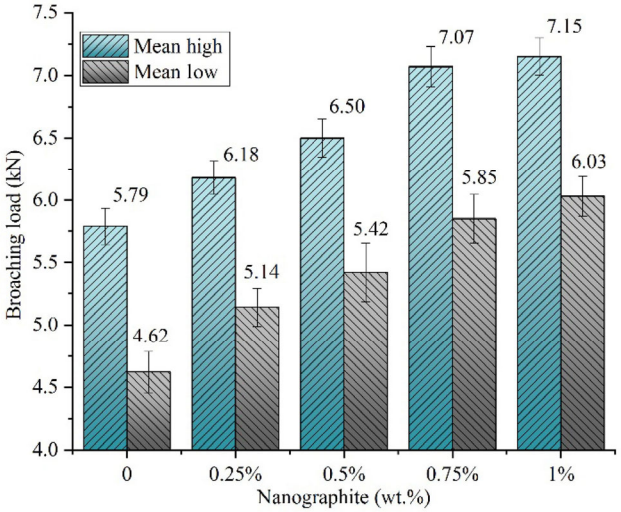


**Fig. 5** Broaching load for different concentrations of nanographite in the WOS-G cutting fluid.

Figure 3 presents the average broaching load of the CCF and W-O. The mean high and mean low broaching loads decreased with increasing concentration of castor oil in the W-O cutting fluids. Note that when the mass fraction of castor oil was 10 wt.%, the minimum mean high and low values of the broaching load were 6.14 kN and 4.9 kN, respectively. Compared with the CCF, there was an approximate reduction of 9.6% and 11.5% in the broaching load due to the cooling and lubrication effects of the cutting fluid, respectively. However, when the mass fraction of castor oil exceeded 10 wt.%, the broaching load no longer significantly decreased. Hence, the dispersion of a certain amount of castor oil in water could benefit broaching to some extent. The dispersed oil was delivered into the limited interface between the cutting edge of the tool and the chip, of which it moved in and out at an equal rate. The dynamic equilibrium of the dispersed castor oil would inhibit a change in its ratio in the W-O fluid. Hence, the optimal concentration for castor oil in the W-O fluid was 10 wt.%.

Based on the optimization of the first type of cutting fluid, the average broaching load for the second type of cutting fluid (WO-S) is shown in Fig. 4. As expected, the mean values at the initial ratio (0.5 wt.%) are slightly higher than those for the optimal W-O fluid. With increasing concentration of LAS in the WO-S cutting fluids, the mean high and low broaching loads decreased first and then increased. The minimum mean high and mean low broaching loads were 5.79 kN and 4.62 kN, respectively, at 1.5 wt.% LAS. It was possible to achieve 17% and 18.5% reduction in both the high and low values, compared to that with 10 wt.% castor oil in the W-O fluid. However, when the LAS exceeded 1.5 wt.%, the broaching load appeared to be stabilized. Owing to the use of this emulsifying agent (LAS), the properties of the cutting fluid were distinctly improved from those of the previous W-O cutting fluid, thereby enabling more oil (and hence, lubrication) to reach the tool-workpiece-chip interface. Hence, increasing the amount of LAS was an effective way of load shedding. However, the reduction will cease once the dynamic equilibrium of the dispersed castor oil with LAS is reached in the confined space. Therefore, an LAS mass fraction of 1.5 wt.% was optimal for addition to the WO-S cutting fluid.

The results for the average broaching load of the third type of WOS-G cutting fluid which was prepared to further optimize the WO-S cutting fluids, were interesting, as shown in Fig. 5. The high and low load values seemed to increase with increasing ratio of nanographite in the WOS-G cutting fluids. The rate of increase of the average broaching load was lower for a nanographite mass fraction exceeding 0.75%. For 1 wt.% of nanographite in the WOS-G cutting fluid, the maximum mean high and low load values were 7.15 kN and 6.03 kN, respectively—much higher than those in the dry broaching condition. Therefore, although the nanographite had good thermal conductivity and lubricating performance, it may not be appropriate for addition to the cutting fluid for broaching.

### 3.2 Physical characteristics of cutting fluids

Stability, density, viscosity, and specific heat are the basic characteristics of cutting fluids. These characteristics represent their service life, internal resistance, and heat and mass transfer performance, and have significant influence on the lubrication, cleaning, and cooling of the cutting zones in the tool, workpiece, and chip.

The long-term stability of the three preferred cutting fluids at room temperature (20 °C) is shown in Fig. 6. All cutting fluids were measured when just prepared. No significant changes were observed in the fluids after 1 day. After standing for 15 days, traces of oil

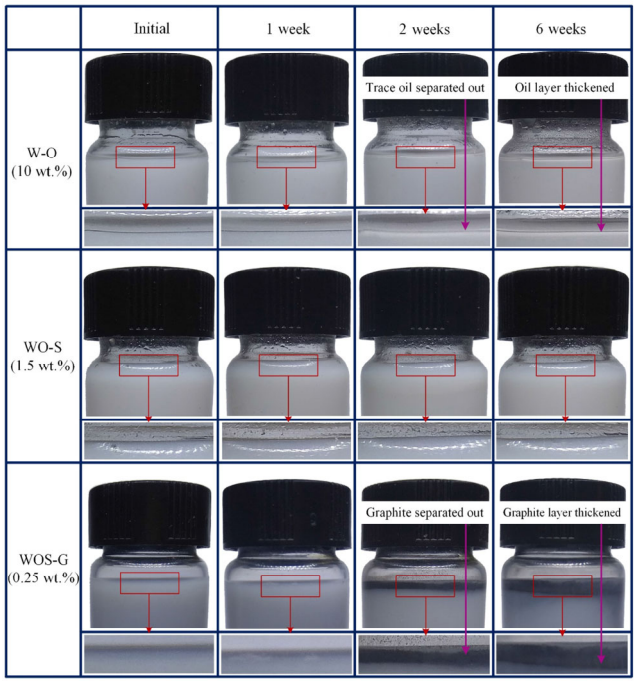


**Fig. 6** Stability of the three preferred cutting fluids at room temperature (20°C).

and nanographite separated from W-O and WOS-G respectively, and were suspended in neck of the bottle; nevertheless, WO-S still showed no marked change. After 30 days, a thicker layer of oil appeared in W-O, and a large amount of nanographite became more visible in WOS-G; nevertheless, the WO-S fluid showed no apparent change. Considering the stratification, the stability of the cutting fluids was deemed to deteriorate in the order of WO-S > W-O > WOS-G.

The experimental densities of the five variants of each type of cutting fluid were similar. The densities of the five variants of W-O varied from 0.998 to 0.990 g/cm$^3$, presenting a tenuous downward tendency with increasing castor oil content from 1 to 20 wt.%. Meanwhile, with increasing LAS content from 0.5 to 2.5 wt.%, the densities of WO-S decreased from 0.989 to 0.985 g/cm$^3$. On the other hand, the addition of nanographite to the WO-S cutting fluid led to a slight increase in the density. The densities of the five variants of WOS-G increased from 0.989 to 0.994 g/cm$^3$ with increasing nanographite content from 0.25% to 1.0% by weight.

The viscosities and specific heats of the five variants of each type of cutting fluid are plotted in Figs. 7–9. In Fig. 7, the specific heats and kinematic viscosities of the W-O cutting fluids exhibited opposite trends with

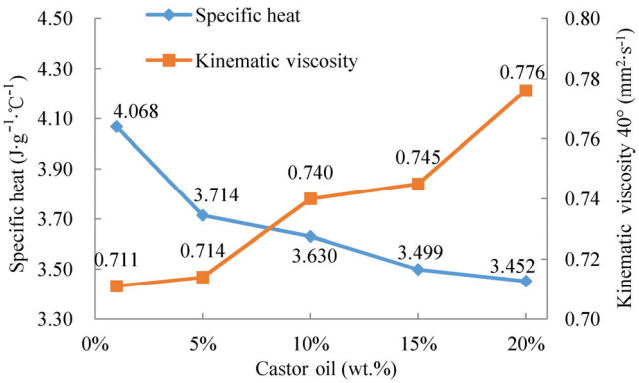


**Fig. 7** Variation in the specific heat and kinematic viscosity of the W-O cutting fluids at 40 °C.

increasing castor oil content from 1 to 20 wt.%. This was attributed to the greater dispersion of oil droplets throughout the continuous phase of water with increasing concentration of castor oil. Castor oil, which is a known source of ricinoleic acid, has a lower specific heat than water. Therefore, the specific heat values decreased from 4.068 to 3.452 J/(g·°C), while the kinematic viscosities at 40 °C increased from 0.711 to 0.776 mm$^2$·s$^{-1}$. In general, a higher content of fatty acid would result in higher viscosity.

LAS is a class of anionic surfactants with long-chain monoalkenes. It can cause micelle formation, in which the lipophilic tails remain inside the oil droplet and the polar heads form a hydrophilic outer layer. These micelles may form a barrier between the oil droplets to prevent the merging of larger droplets. In the WO-S cutting fluid, it was observed in Fig. 8 that the specific heat and kinematic viscosity exhibited two different trends, i.e., convexity and concavity, with increasing LAS content from 0.5% to 2.5% for the same castor oil concentration. The specific heat values first

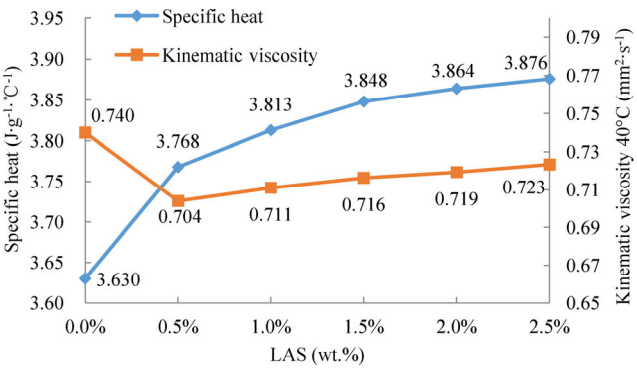


**Fig. 8** Variation in the specific heat and kinematic viscosity of WO-S cutting fluids at 40 °C.

increased rapidly from 3.630 J/(g·°C), then slowly to 3.876 J/(g·°C). The kinematic viscosity values first decreased rapidly from 0.740 to 0.704 $mm^2 \cdot s^{-1}$ and then increased slowly to 0.723 $mm^2 \cdot s^{-1}$. This may be related to the increasing ionic strength of the more dispersed micelles.

With increasing nanographite content, the opposite trend was observed in Fig. 9. The specific heat and kinematic viscosity of the WOS-G cutting fluid exhibited opposite trends with increasing nanographite content from 0.25 to 1.0 wt.%. The specific heats increased from 3.848 to 4.115 J/(g·°C), while the kinematic viscosities decreased from 0.733 to 0.679 $mm^2 \cdot s^{-1}$. Therefore, to a certain extent, nanographite may consume some of the castor oil and LAS.

### 3.3 Wettability and permeability of cutting fluids

The wettability and permeability of cutting fluids play a dominant role in lubrication on the surface of the workpiece and tool, provided the cutting parameters (excluding the cutting speed) are maintained constant during broaching. Meanwhile, the atomization of the cutting fluids with the nozzle decreases the supplied liquid quantity per unit time, thereby reducing the wetting and permeation abilities into the workpiece and tool substrates. In this study, the wetting angle and its variation were chosen to evaluate the wettability and permeability of the three types of cutting fluids. As the wetting angles and their variation among the five variants of each type of cutting fluid were similar, W-O (10 wt.%), WO-S (1.5 wt.%), and WOS-G (0.5 wt.%) were chosen as representatives. The wetting angles and corresponding variation in the three types of cutting fluids on the workpiece and tool were recorded using a KEYENCE VW-9000 high-speed microscope and are presented in Fig. 10.

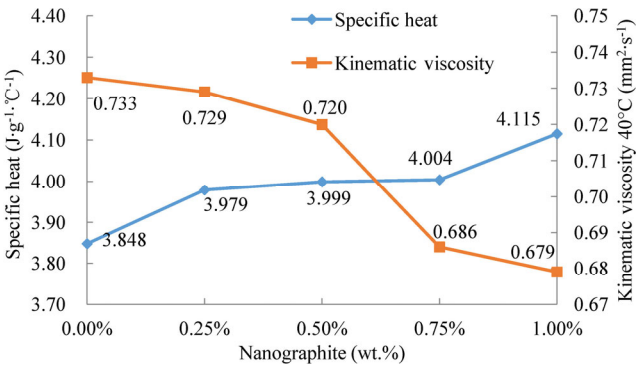


**Fig. 9** Variation in the specific heat and kinematic viscosity of WOS-G cutting fluids at 40 °C.

As shown in Fig. 10(a), when $t$ = 0, on the workpiece surface, W-O exhibits the maximum wetting angle of 81.17°, while WO-S exhibits the minimum wetting angle of 74.27°. After 2 s from the first contact time, W-O still exhibits the largest wetting angle of 68.29°, while WO-S exhibits the smallest wetting angle of 53.96°. Moreover, within the first 2 s, the largest variation in the wetting angle of 20.31° occurs on WO-S. Variations in the wetting angles for W-O and WOS-G were 12.88° and 11.86°, respectively. This implies that WO-S had the best wettability and permeability on the workpiece.

Likewise, the spreading of the cutting fluids within 2 s after first contact on the broach substrate is shown in Fig. 10(b). At the initiation of impingement of the droplet, W-O exhibited the largest wetting angle of 85.82°, while WO-S exhibited the smallest wetting angle of 79.83°. When $t$ = 2 s, W-O presented the largest wetting angle of 73.17°, while WO-S showed the smallest wetting angle of 61.24°. The rapid spreading

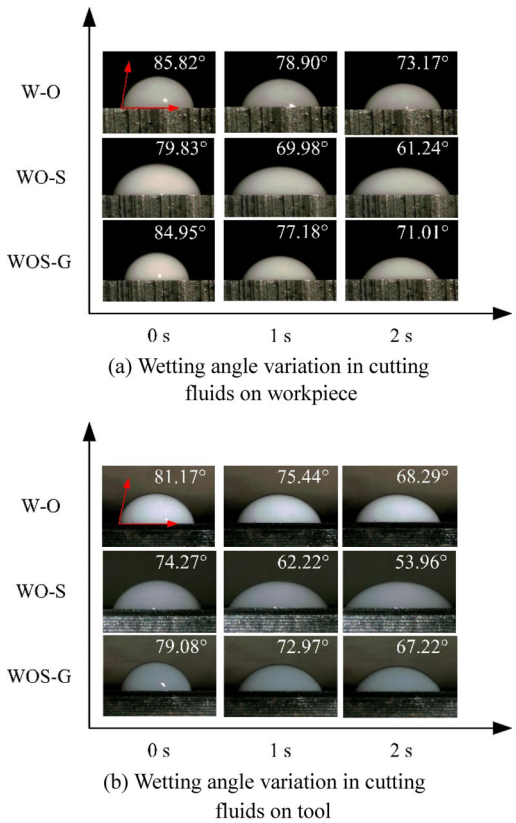


**Fig. 10** Wetting angle variation in different types of cutting fluids on different substrates.

of the different types of cutting fluids is also reflected in the graph. As seen from Fig. 10(b), wetting rate, 18.59° variation within 2 s, occurred much faster in the WO-S cutting fluid than that in both W-O and WOS-G cutting fluids, 12.65° and 13.94° variations within 2 s. This further confirmed the optimum wettability and permeability of WO-S on the tool. As already demonstrated, WO-S had the best wettability and permeability on the tool and workpiece. The wettability and permeability of W-O and WOS-G were relatively poor and not much different.

## 4 Mechanism analysis of cutting fluids

### 4.1 Influence of castor oil on broaching performance

As per the experimental results for the broaching load reported in previous sections (Fig. 3), increasing additive concentration of castor oil led to the reduction of broaching load due to the sufficient lubrication and cooling. Hence, castor oil is a satisfactory additive in eco-friendly water-based cutting fluids for broaching. Although castor oil could greatly benefit broaching, its influence should be considered further from the theoretical point of view for more applications.

Figure 11 shows the micrograph of the droplet size distribution in the W-O cutting fluid after ultrasonic agitation. The W-O cutting fluid contained a dispersed oil phase and a continuous water phase, i.e., oil-in-water. The oil droplets had a maximum diameter of less than 5 μm. These miniscule oil-in-water droplets were more likely to adhere to the surface of the tool and workpiece, enabling their entry into the slit area of the tool-workpiece-chip. Hence, the broaching load was effectively reduced as the lubrication and cooling effects were greatly enhanced.

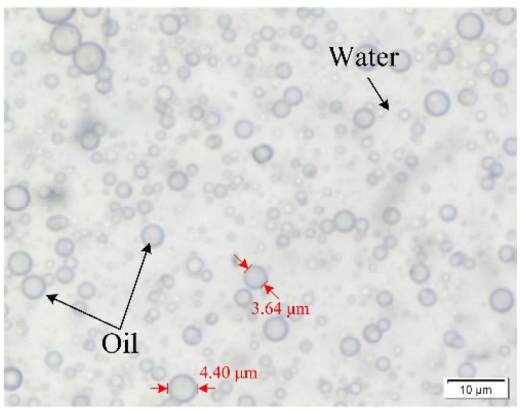


**Fig. 11** Micrograph of droplet size distribution in W-O (10 wt.%) cutting fluids.

Secondly, those evident results could be attributed to triglycerides, which are a major component of castor oil. Triglycerides have glycerol molecules with three long-chain fatty acids attached to the hydroxyl groups through ester linkages. These fatty acids cause hydrolysis in castor oil. Figure 12 shows the lubrication mechanism of the castor oil-in-water fluid. In general, ricinoleic acid is hydrolyzed to ricinoleic acid with -COOH and glycerol ($C_3H_8O_3$). The polar group –COOH is well-adsorbed onto the surface of the tool-workpiece-chip by virtue of the van der Waals force between the atom and molecule. This creates a film of the adsorbate, a monomolecular layer, or multimolecular layer with orientation arrangement structure, thereby separating the tool-workpiece-chip surface. This mechanism is typically classified as physisorption, by which a low shear resistance interface can effectively reduce the contact adherence and friction between the surfaces. Moreover, as the other product of hydrolysis [25], glycerol also has very good lubricating ability, further enhancing the effect of castor oil.

### 4.2 Influence of LAS on broaching performance

As per the results in Fig. 4, LAS is another beneficial additive for eco-friendly water-based cutting fluids in broaching. Hence, the effect of LAS in the WO-S cutting fluid should be analyzed.

Figure 13 shows the micrograph of the droplet size distribution in the WO-S cutting fluid obtained after ultrasonic agitation. The oil-in-water characteristic is more pronounced. Compared with the W-O cutting

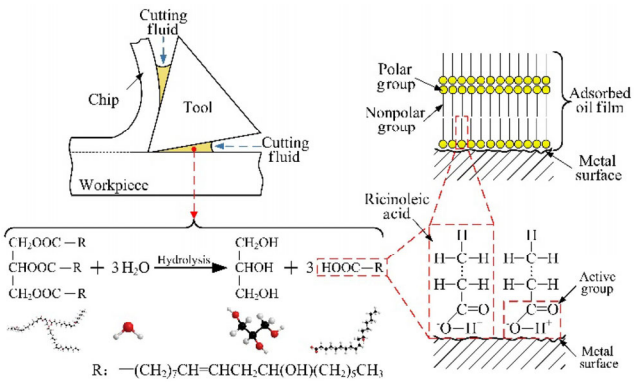


**Fig. 12** Lubrication mechanism of castor oil-in-water fluid.

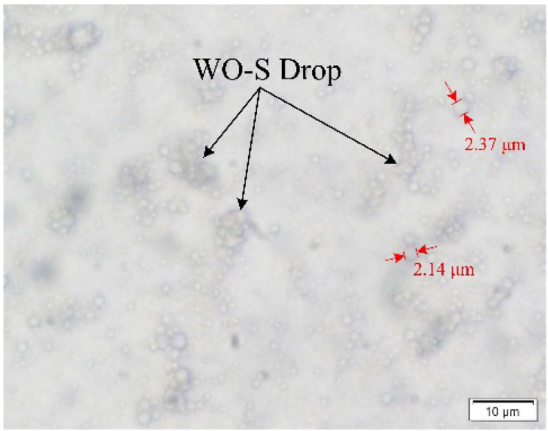


**Fig. 13** Micrograph of droplet size distribution in WO-S (1.5 wt.%) cutting fluids.

fluid (Fig. 13), castor oil, with a droplet size below approximately 3 μm, is more finely and uniformly dispersed under the action of LAS. These large amounts of micro oil-in-water droplets are active ingredients for lubrication, and are more likely to penetrate the surface of the tool-workpiece-chips. Hence, the broaching load was further effectively reduced.

Secondly, this advantage resorted to the excellent wettability and permeability of the cutting fluid WO-S. Figure 10 shows that WO-S could lubricate the cutting edge of the broaching tool to release the cutting forces, owing to their best wettability and permeability on the tool and workpiece among the three types of cutting fluids. Moreover, WO-S could clean the surface of the cutting edge of the broaching tool to protect it from wear by microchips. The cleaning mechanism is illustrated in Fig. 14. When the atomized cutting fluid entered the cutting zone of the tool-workpiece-chip, due to the wetting and permeating action of the surfactant molecules, the hydrophilic base in the cutting fluid penetrated the surface between the micro-cutting chips and tool, thereby weakening the adhesion of the micro-cutting chips. Subsequently, due to the emulsification and dispersion of the surfactant molecules, the micro-cutting chips were surrounded by lipophilic groups to form a large suspension that could be easily cleaned away. Simultaneously, the surface of the broaching tool was covered by surfactant molecules which inhibited the re-deposition of the micro-cutting chips. Hence, the broaching load was effectively reduced as the lubrication and cooling effects were greatly enhanced.

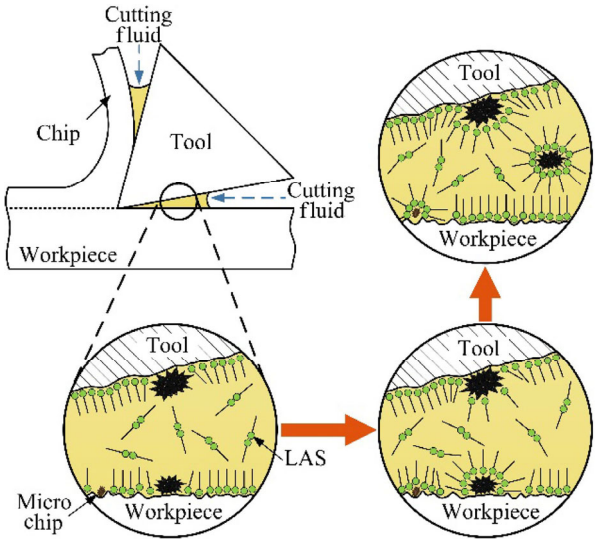


**Fig. 14** Cleaning mechanism of micro-cutting chips on the cutting edge of broaching tool.

### 4.3 Influence of nanographite on broaching performance

Figure 5 shows that although the addition of nanographite to WOS-G could not reduce the broaching load, it had good thermal and lubricating properties. Hence, the positive effect of nanographite on broaching was the smallest, and sometimes even negative.

Agglomeration of nanographite in the WOS-G cutting fluid occurred. Nanographite was thermodynamically unstable because of its layered, planar structure, and hence, could bond readily and form multiple stable covalent bonds under the suitable agglomeration of multivalent carbon (Fig. 15). Moreover, nanographite and castor oil bonded owing to their similar polarities.

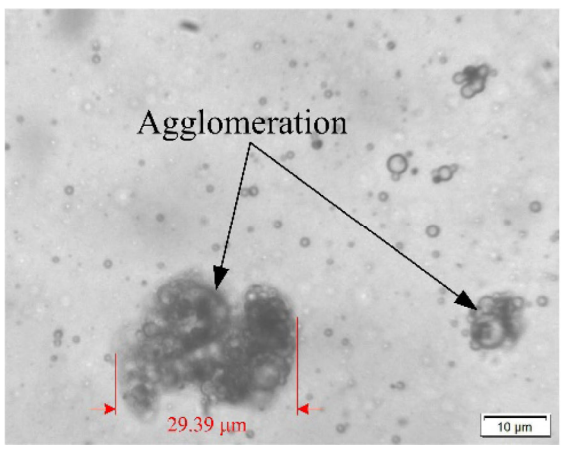


**Fig. 15** Micrograph of droplet size distribution in WOS-G (0.5 wt.%) cutting fluids.

Finally, LAS reduced the oil-water surface tension and further accelerated the growth and agglomeration of the droplets. The maximum diameter of the oil-in-water droplet was 10 μm. The agglomeration of nanographite significantly mitigated the lubrication and cooling of the WOS-G cutting fluid, because the agglomeration disturbed the uniform distribution of the surfactant and nanographite in fluid, and overrode the benefits offered by the nanographite and surfactant.

## 5 Conclusions

(1) Comparing the broaching loads obtained using different concentrations of castor oil and CCF, 10 wt.% castor oil could reduce more than 10% of the broaching load in broaching. Castor oil is therefore a beneficial and eco-friendly additive for water-based cutting fluids (W-O).

(2) Use of the WO-S cutting fluid in the MQL technology resulted in the lowest broaching load in this study. Owing to its excellent cooling, lubrication, and cleaning performance, WO-S could lubricate and cool the cutting edge to decrease the cutting load, and clean the surface of the cutting edge to keep it sharp. The optimal concentration of LAS in this experiment was 1.5 wt.% (mass fraction).

(3) Nanographite is not recommended as a beneficial additive for water-based cutting fluids (WOS-G). When castor oil, LAS, and nanographite were added simultaneously, nanographite underwent serious agglomeration, resulting in a significant reduction in the lubrication.

## Acknowledgements

This research is supported by National Natural Science Foundation of China (Grant No. 51775153).



## References

[1] Lee C M, Choi Y H, Ha J H, Woo W S. Eco-friendly technology for recycling of cutting fluids and metal chips: A review. *Int J Precis Eng Manuf Green Technol* **4**(4): 457–468 (2017)

[2] Wang H, Huang L J, Yao C, Kou M, Wang W Y, Huang B H, Zheng W Z. Integrated analysis method of thin-walled turbine blade precise machining. *Int J Precis Eng Manuf* **16**(5): 1011–1019 (2015)

[3] Shin D H, Lee S, Jeong C P, Kwon O S, Park T S, Jin S H, Ban D H, Yang S H. Analytic approaches for keeping high braking efficiency and clamping efficiency of electro wedge brakes. *Int J Precis Eng Manuf* **16**(7): 1609–1615 (2015)

[4] Debnath S, Reddy M M, Yi Q S. Environmental friendly cutting fluids and cooling techniques in machining: A review. *J Clean Prod* **83**: 33–47 (2014)

[5] Xavior M A, Adithan M. Determining the influence of cutting fluids on tool wear and surface roughness during turning of AISI 304 austenitic stainless steel. *J Mater Process Technol* **209**(2): 900–909 (2009)

[6] Sarıkaya M, Güllü A. Multi-response optimization of minimum quantity lubrication parameters using Taguchi-based grey relational analysis in turning of difficult-to-cut alloy Haynes 25. *J Clean Prod* **91**: 347–357 (2015)

[7] Belluco W, De Chiffre L. Testing of vegetable-based cutting fluids by hole making operations. *Lubr Eng* **57**: 12–16 (2001)

[8] Belluco W, De Chiffre L. Surface integrity and part accuracy in reaming and tapping stainless steel with new vegetable based cutting oils. *Tribol Int* **35**(12): 865–870 (2002)

[9] Burton G, Goo C S, Zhang Y Q, Jun M B G. Use of vegetable oil in water emulsion achieved through ultrasonic atomization as cutting fluids in micro-milling. *J Manuf Process* **16**(3): 405–413 (2014)

[10] Li B K, Li C H, Zhang Y B, Wang Y G, Jia D Z, Yang M. Grinding temperature and energy ratio coefficient in MQL grinding of high-temperature nickel-base alloy by using different vegetable oils as base oil. *Chin J Aeronaut* **29**(4): 1084–1095 (2016)

[11] Wang Y G, Li C H, Zhang Y B, Yang M, Li B K, Dong L, Wang J. Processing characteristics of vegetable oil-based nanofluid MQL for grinding different workpiece materials. *Int J Precis Eng Manuf Green Technol* **5**(2): 327–339 (2018)

[12] Shokoohi Y, Khosrojerdi E, Shiadhi B H R. Machining and ecological effects of a new developed cutting fluid in combination with different cooling techniques on turning operation. *J Clean Prod* **94**: 330–339 (2015)

[13] Bataller H, Lamaallam S, Lachaise J, Graciaa A, Dicharry C. Cutting fluid emulsions produced by dilution of a cutting fluid concentrate containing a cationic/nonionic surfactant mixture. *J Mater Process Technol* **152**(2): 215–220 (2004)

[14] Cambiella A, Benito J M, Pazos C, Coca J, Hernández A, Fernández J E. Formulation of emulsifiable cutting fluids and extreme pressure behaviour. *J Mater Process Technol* **184**(1–3): 139–145 (2007)

[15] John J, Bhattacharya M, Raynor P C. Emulsions containing vegetable oils for cutting fluid application. *Colloids Surf A Physicochem Eng Aspects* **237**(1–3): 141–150 (2004)

[16] Adamczuk K, Legutko S, Laber A, Serwa W. Investigation of the influence of coolant-lubricant modification on selected effects of pull broaching. In *Proceedings of the 3rd International Conference Energy, Environment and Material Systems*, Olanica-Zdrój, 2017: 1–5.

[17] Sukirno, Ningsih Y R. Utilization of sulphurized palm oil as cutting fluid base oil for broaching process. In *Proceedings of the 1st International Symposium on Green Technology for Value Chains*, Tangerang, Bristol, 2017: 1–11.

[18] Krishna P V, Srikant R R, Rao D N. Experimental investigation on the performance of nanoboric acid suspensions in SAE-40 and coconut oil during turning of AISI 1040 steel. *Int J Mach Tools Manuf* **50**(10): 911–916 (2010)

[19] Zareh-Desari B, Davoodi B. Assessing the lubrication performance of vegetable oil-based nano-lubricants for environmentally conscious metal forming processes. *J Clean Prod* **135**: 1198–1209 (2016)

[20] Chu B, Singh E, Koratkar N, Samuel J. Graphene-enhanced environmentally-benign cutting fluids for high-performance micro-machining applications. *J Nanosci Nanotechnol* **13**(8): 5500–5504 (2013)

[21] Ni J, Feng G D, Meng Z, Hong T, Chen Y B, Zheng X. Reinforced lubrication of vegetable oils with graphene additive in tapping ADC12 aluminum alloy. *Int J Adv Manuf Technol* **94**(1–4): 1031–1040 (2018)

[22] Maruda W R, Legutko S, Krolczyk G M. Influence of minimum quantity cooling lubrication (MQCL) on chip formation zone factors and shearing force in turning AISI 1045 steel. *Appl Mech Mater* **657**: 43–47 (2014)

[23] Uysal A, Demiren F, Altan E. Applying minimum quantity lubrication (MQL) method on milling of martensitic stainless steel by using nano $Mos_2$ reinforced vegetable cutting fluid. *Proced Social Behav Sci* **195**: 2742–2747 (2015)

[24] Klocke F, Settineri L, Lung D, Priarone P C, Arft M. High performance cutting of gamma titanium aluminides: Influence of lubricoolant strategy on tool wear and surface integrity. *Wear* **302**(1–2): 1136–1144 (2013)

[25] Shi Y J, Minami I, Grahn M, Björling M, Larsson R. Boundary and elastohydrodynamic lubrication studies of glycerol aqueous solutions as green lubricants. *Tribol Int* **69**: 39–45 (2014)

**Jing NI.** He received his M.S. and Ph.D. degrees in mechanical and engineering from Zhejiang University, China, in 2003 and 2006, respectively. He joined Hangzhou Dianzi University from 2006. His current position is a professor and dean of the School of Mechanical and Engineering. His research areas cover lubrication and cooling of cutting tool with green fluids and green additives such as nano-particles and surfactants.

**Lihua HE.** He received his M.S. and Ph.D. degrees in mechanical engineering from Hunan University, China, in 2012 and 2017, respectively. He joined Hangzhou Dianzi University from 2017. His research interests include precision machining and green manufacturing based on nanotechnology.